Laser Controlled Tunneling in a Vertical Optical Lattice

Q. Beaufils, G. Tackmann, X. Wang, B. Pelle, S. Pelisson, P. Wolf, and F. Pereira dos Santos*

LNE-SYRTE, Observatoire de Paris, LNE, CNRS, UPMC; 61 avenue de l'Observatoire, 75014 Paris, France

Raman laser pulses are used to induce coherent tunneling between neighboring sites of a vertical 1D optical lattice. Such tunneling occurs when the detuning of a probe laser from the atomic transition frequency matches multiples of the Bloch frequency, allowing for a spectroscopic control of the coupling between Wannier-Stark (WS) states. In particular, we prepare coherent superpositions of WS states of adjacent sites, and investigate the coherence time of these superpositions by realizing a spatial interferometer. This scheme provides a powerful tool for coherent manipulation of external degrees of freedom of cold atoms, which is a key issue for quantum information processing.

PACS numbers: 32.80.Qk, 05.60.Gg, 37.10.Jk, 37.25.+k

Trapping and manipulating cold neutral atoms in an optical lattice offers high controllability and robust quantum coherence properties, which makes it an attractive system for many applications such as quantum simulation of solid state systems [1], metrology [2,3], and quantum information processing (QIP) [4]. One key issue in this context is the possibility to coherently control the atoms internal and external degrees of freedom. Combined with the possibility to address single sites [5], this allows for the realization of quantum logic operations [6].

Atom transport control in an optical lattice has been previously reported using microwave fields [7], frequency, phase and amplitude modulation techniques [8–10], or an adiabatic change of the trapping potential [11,12]. In this work, we demonstrate coherent laser induced tunneling of cold atoms between neighboring sites of an optical lattice. In contrast with most previous approaches, our technique does not require any modification of the trapping potential. It allows us to displace the atoms by a large number of lattice periods (up to 9 in this work) in a system showing good coherence properties (up to 1 s).

Our system consists of laser-cooled ^{87}Rb atoms in the first band of a vertical one-dimensional optical lattice. Because of earth gravity, the ground energy levels of each site of the lattice are shifted out of resonance. For a sufficiently large lattice depth U_l, tunneling is highly reduced, leading to a ladder of localized Wannier-Stark (WS) eigenstates separated by the Bloch frequency $\nu_B = m_a g \lambda_l / 2h$. Here, m_a is the atomic mass, g is the gravity acceleration, $\lambda_l / 2$ is the distance between two adjacent lattice sites, and h is the Planck constant. The WS states $|W_m\rangle$ are indexed by the discrete quantum number m characterizing the well containing the center of the wave function $\langle x | W_m \rangle$. The observation of Bloch oscillations of the atoms in such a system have already been reported and allowed a precise measurement of the Bloch frequency [13,14].

We use counterpropagating Raman beams to drive coherent transitions between the ground and excited

hyperfine levels $|g\rangle = |5^2 S_{1/2}, F = 1, m_F = 0\rangle$ and $|e\rangle = |5^2 S_{1/2}, F = 2, m_F = 0\rangle$. Such a transition implies a momentum transfer of $k_{\text{eff}} = k_1 + k_2 \approx 4\pi/(780 \text{ nm})$ that couples the WS states either in the same well or in neighboring wells, with a coupling strength proportional to $\langle W_m | e^{ik_{eff}x} | W_{m\pm\Delta m} \rangle$. Fourier-limited widths of the resonances over excitation times larger than the Bloch period allows resolved intersite transitions $|g, m\rangle \rightarrow |e, m \pm \Delta m\rangle$, at Raman frequencies

$$\nu_R = \nu_{\text{HFS}} \pm \Delta m \times \nu_B,$$

where ν_{HFS} is the hyperfine splitting and Δm is the number of lattice wells separating the two coupled WS states. The energy spectrum of our system is schematically illustrated in Fig. 1.

Coupling between neighboring wells can be efficiently tuned using the lattice depth when k_l is close to k_{eff}, where k_l is the optical lattice wave vector [15]. We therefore use a mixed trap configuration with a blue detuned lattice generated by a single mode frequency doubled Nd: YVO$_4$ laser ($\lambda_l = 532$ nm, beam waist 600 μm) that provides only vertical longitudinal confinement, superposed with a
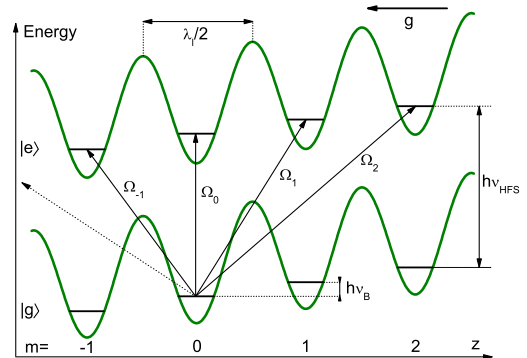

FIG. 1 (color online). Atoms in the first band of the lattice form a Wannier-Stark ladder of eigenstates. The Raman probe laser couples the ground to the excited hyperfine level in the different WS states separated by the Bloch frequency.

red detuned ($\lambda = 1064$ nm, beam waist 200 μm) Yb fiber laser providing transverse confinement (see Fig. 2). To load this dipole trap, we superimpose it to a 3D-Magneto-Optical trap (MOT) containing 10^7 atoms fed by a 2D-MOT during 500 ms. The cloud is then cooled down to 2 μK by a far detuned molasses, at the end of which we switch off the cooling lasers to let the untrapped atoms fall. At our low lattice depth ($U_l \simeq 4E_R$ (where $E_R = (\hbar k_l)^2/(2m_a)$ is the lattice recoil energy), only the first band has a non-negligible lifetime and is populated with about 10^5 atoms vertically distributed along 10^4 sites (the second band is centered at $5E_R$ already above the lattice depth). The atoms accumulated in all the Zeeman sublevels of $|5^2S_{1/2}, F = 2\rangle$ are depumped to $|5^2S_{1/2}, F = 1\rangle$ and then optically pumped (95% efficiency) on the $|5^2S_{1/2}, F = 1\rangle \rightarrow |5^2P_{3/2}, F = 0\rangle$ transition to the $|5^2S_{1/2}, F = 1, m_F = 0\rangle$ Zeeman sublevel, which is sensitive to stray magnetic fields only to second order. The remaining 5% unpolarized atoms can easily be removed from the trap with a pushing beam. Our fluorescence detection scheme, based on a time of flight measurement similar to the one used in atomic clocks and inertial sensors, allows us to measure the atomic populations in the two hyperfine states after releasing the atoms from the trap [16]. The Raman transitions are driven by two counterpropagating beams at 780 nm circularly polarized, detuned from the atomic transition by about 3 GHz, and aligned along the direction

of the optical trap beams. The beams are collimated with a $1/e^2$ radius of 1 cm, ensuring a good intensity homogeneity along the transverse size of the trap (about 200 μm radius).

Figure 3 shows two typical Raman spectra of the transition probability as a function of the Raman frequency ν_R, taken for two different lattice depths. Transitions between the two hyperfine levels at Raman frequencies equal to the hyperfine splitting plus or minus an integer number Δm of Bloch frequencies ($\nu_B \approx 569$ Hz in our system) are the signature that the atoms actually tunneled across Δm lattice sites. For those scans, the intensities in the Raman laser beams were 0.25 and 0.54 mW/cm^2. The resulting Rabi frequencies $\Omega_{\Delta m}$, different for each transition, are always smaller than the Bloch frequency, so that each peak is well resolved. The ratio between the Raman intensities was chosen to cancel the differential light shift of the hyperfine transition induced by them [17]. The Rabi frequency for each transition Δm is written [18]

$$\Omega_{\Delta m} = \Omega_{U_l=0}\langle W_m|e^{-ik_{\mathrm{eff}}x}|W_{m\pm\Delta m}\rangle, \qquad (1)$$

where $\Omega_{U_l=0}$ is the Rabi frequency in free space. Because of the translational symmetry of the WS states, $\Omega_{\Delta m}$ does not depend on the initial well index m but only on the absolute value of Δm [18]. It also depends on the lattice wavelength λ_l and depth U_l, which is an important feature of this experiment, as it induces a spatial inhomogeneity on the Rabi frequency seen by the trapped atoms via the transverse inhomogeneity of the lattice depth in the trap. The damping induced on the Rabi oscillations by this
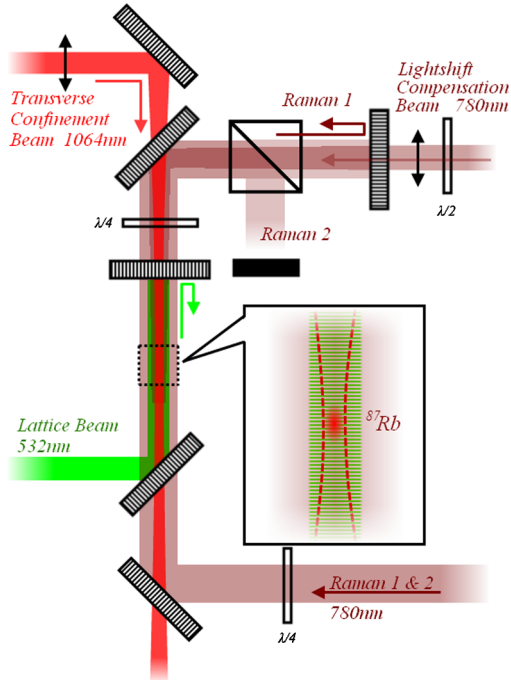

FIG. 2 (color online). Experimental setup for the optical trapping and Raman intersite transitions. The different beams are superposed using dichroic mirrors. The Raman beams are also superposed and one of them is retro-reflected to allow counterpropagating transitions.
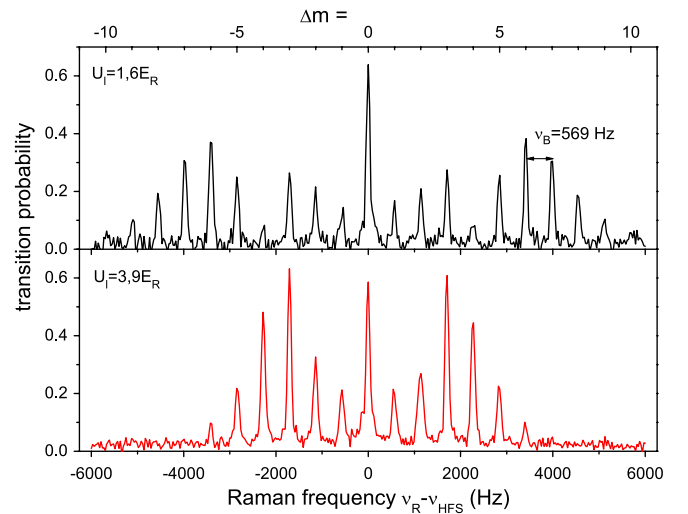

FIG. 3 (color online). Raman spectra for two different lattice depths, showing evidence of transitions between up to 9 neighboring lattice sites, each having a different Rabi frequency according to Eq. (1). The excitation time is 10 ms, which is smaller than the duration of a π pulse for each transition. The peaks are separated by the Bloch frequency of our system $\nu_B \approx 569$ Hz, and their amplitudes are related to the Rabi frequencies calculated in Fig. 4.

inhomogeneity is the main limitation on the transfer efficiency of the Raman transitions.

We calculated $\Omega_{\Delta m}$ for the parameters of our system, as a function of U_l and for various values of Δm. The result is shown in Fig. 4 for $\Delta m = \pm 1$, $\Delta m = \pm 2$ and $\Delta m = \pm 3$. To limit the lattice depth inhomogeneity due to the transverse extension of the atomic cloud, the $1/e^2$ waist of the beam providing transverse confinement is smaller than the one of the lattice beam. Moreover, we can choose to tune the lattice depth at a value where, for a transition of interest, the variation of the coupling with lattice depth $\Delta\Omega(U_l)/\Delta U_l$ is small, as illustrated by the inset of Fig. 4. On this graph, we compare the shape of Rabi oscillations at resonance for the $\Delta m = -3$ transition and for two different lattice depths. Besides a difference in the period of the Rabi oscillations, we observe that the best contrast is obtained for $U_l \simeq 4E_R$, where the coupling inhomogeneity is lower, allowing us to reach a transfer efficiency of about 80%. The lattice depth is estimated by measuring the Rabi frequencies for different transitions and comparing them to the calculation.

We investigated the question of the coherence time of the trapped states. As a diagnosis tool, we performed Ramsey spectroscopy on the $|g, m\rangle \rightarrow |e, m+3\rangle$ transition. As there is no initial atomic coherence from one site to the neighboring site, the atoms distributed in many lattice sites can be treated as independent interferometers. The phase is read out by the measurement of the internal atomic state population. Our interferometer consists in two Raman $\pi/2$ pulses of frequency ν_R scanned close to $\nu_{HFS} + 3\nu_B$, separated by a time interval T (see inset of Fig. 5). The intensity of the Raman lasers was chosen for the Rabi frequency $\Omega_{\Delta m=3}/2\pi$ to be much smaller than ν_B, in order to ensure a good separation with neighboring transitions. The duration of the $\pi/2$ pulses is then $\tau_{\pi/2} = 5.5$ ms. Figure 5 shows as open circles the evolution of the
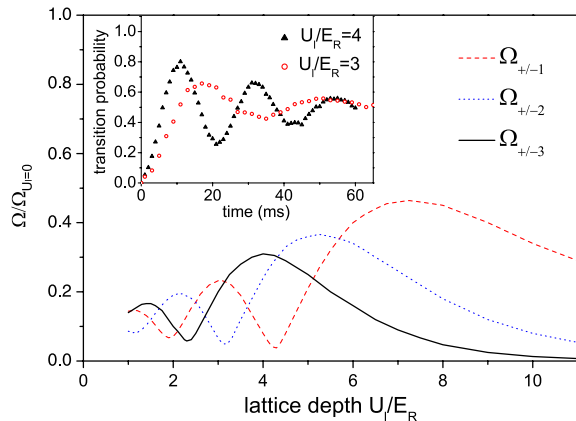
contrast as we increase the interrogation time T. The contrast at short T is about 60%, which is coherent with the 80% efficiency of each of the two Raman $\pi/2$ pulses. When increasing T, the contrast decreases rapidly, which is due to the transverse inhomogeneity of the differential light shift induced on the hyperfine transition by the Gaussian profile of the IR laser used for transverse trapping [19]. This position dependent frequency shift induces an inhomogeneous broadening along the transverse direction, which is the main effect limiting the coherence lifetime in the lattice trap.

Many schemes have been proposed and demonstrated to cancel this source of inhomogeneous dephasing in an optical trap [20–22]. One particularly efficient method in our case is to add a low power laser beam, mode matched with the transverse trapping beam, and whose frequency is tuned between the two hyperfine levels, as reported in [23]. This beam compensates the differential lightshift induced by the transverse trapping light with a laser power of only a few tens of nW, so that decoherence due to photon scattering is negligible at the experiment's time scale. In practice, we use as a compensating beam a fraction of one of the two Raman beams, with an additional detuning of 80 MHz in order to prevent undesired Raman transitions. This beam is superposed with the IR laser (see Fig. 2), and its size, position and power are adjusted to optimize the contrast of the interferometer for long interrogation times of several hundreds of milliseconds, for which otherwise the contrast is zero. In our case, for an IR power of about 2 W, the differential light shift is compensated with a power of 12 nW. Figure 5 displays as black squares the evolution of the contrast vs T with the compensating beam, and clearly shows the improvement of the lifetime of the coherence.

Finally, as a preliminary investigation, we evaluated the frequency sensitivity of the interferometer. This is
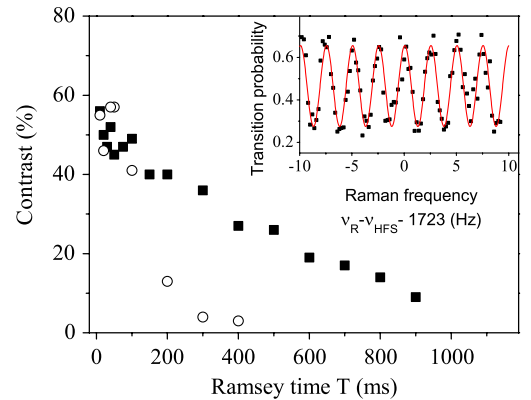

FIG. 4 (color online). Calculation of the normalized Rabi frequencies for $\Delta m = \pm 1$, $\Delta m = \pm 2$ and $\Delta m = \pm 3$ transitions, as a function of the lattice depth. Inset : Experimental Rabi oscillations on the transition $\Delta m = -3$, for $U_l = 4E_R$ and $U_l = 3E_R$.

FIG. 5 (color online). Contrast of the interferometer versus Ramsey interrogation time T. Open circles (black squares) display the contrast without (with) the light shift compensation beam. Inset: Corresponding typical interference fringes for an interrogation time of 400 ms. The solid line is a least-squares sinusoidal fit to the data.

motivated by the possibility to use this trapped atomic spatial interferometer for metrology applications such as gravimetry or short range forces measurement [24]. We locked the Raman lasers frequency difference to the center fringe of the interferometer, with a computer controlled servo integrator. Performing the measurement alternatively on the left and right transitions ($\Delta m = \pm 3$) and calculating the difference of the measured frequencies allows us to measure $6\nu_B$ while cancelling the frequency shifts of the hyperfine clock frequency, due to, for example, the quadratic Zeeman effect and the differential lightshifts induced by the trapping lasers. For an interrogation time of $T = 400$ ms and a cycle time of $T_c = 1.4$ s, the Allan standard deviation of the frequency difference decreases as 0.1 Hz $\times \tau^{-1/2}$ with τ the integration time in seconds. This corresponds to a statistical uncertainty on the measurement of the Bloch frequency of 6×10^{-5} in relative value after 1 s integration which is about 5 times above the best sensitivity achieved with trapped atoms reported in [25].

If used for a measurement of g, this result is not competitive with free falling cold atoms gravimeters [26]. Nevertheless, the geometry of this trapped interferometer makes it promising for the measurement of short range forces (Casimir-Polder, short range modifications of gravity). Provided the possibility to initially select the atoms in a single lattice site [27] and to reach the same level of sensitivity on ν_B, performing the Wannier-Stark interferometer close to the reflecting surface of the lattice as proposed in [15] would allow a statistical uncertainty in the measurement of the Casimir-Polder potential of 1% for a distance of 5 μm and a measurement time of 1000 s.

In conclusion, we demonstrated a new versatile technique for controlled coherent transport of atoms in a lattice. The high resolution reachable by the Raman transitions (up to 1 Hz) suggests the possibility of selectively addressing one single lattice site, using, for example, the lightshift induced by a focused laser to lift the degeneracy between the transitions. Although demonstrated here for a thermal cloud in a shallow lattice, this technique is also suitable for degenerate quantum gases in deeper lattices (up to about 20 recoil energies). Besides, it also works with one photon transitions, as recently highlighted in [28]. All these features make this tool a potential candidate for the realization of quantum logic operations.

This research is carried on within the project iSense, which acknowledges the financial support of the Future

*franck.pereira@obspm.fr

[1] J. J. Garcia-Ripoll, M. A. Martin-Delgado, and J. I. Cirac, Phys. Rev. Lett. **93**, 250405 (2004).
[2] M. Takamoto, F.-L. Hong, R. Higashi, and H. Katori, Nature (London) **435**, 321 (2005).
[3] P. Cladé et al., Phys. Rev. Lett. **96**, 033001 (2006).
[4] H. J. Briegel et al., J. Mod. Opt. **47**, 415 (2000).
[5] D. Schrader et al., Phys. Rev. Lett. **93**, 150501 (2004).
[6] G. K. Brennen, C. M. Caves, P. S. Jessen, and I. H. Deutsch, Phys. Rev. Lett. **82**, 1060 (1999).
[7] L. Förster et al., Phys. Rev. Lett. **103**, 233001 (2009).
[8] M. Ben Dahan et al., Phys. Rev. Lett. **76**, 4508 (1996).
[9] S. R. Wilkinson et al., Phys. Rev. Lett. **76**, 4512 (1996).
[10] V. V. Ivanov et al., Phys. Rev. Lett. **100**, 043602 (2008).
[11] O. Mandel et al., Nature (London) **425**, 937 (2003).
[12] M. Anderlini et al., Nature (London) **448**, 452 (2007).
[13] G. Roati et al., Phys. Rev. Lett. **92**, 230402 (2004).
[14] P. Cladé et al., Europhys. Lett. **71**, 730 (2005).
[15] F. Pereira dos Santos et al., Proceedings of the 7th Symposium Frequency Standards and Metrology (World Scientific, Singapore, 2009), p. 44.
[16] J. Le Gouët et al., Appl. Phys. B **92**, 133 (2008).
[17] D. S. Weiss, B. C. Young, and S. Chu, Appl. Phys. B **59**, 217 (1994).
[18] P. Lemonde and P. Wolf, Phys. Rev. A **72**, 033409 (2005).
[19] S. Kuhr et al., Phys. Rev. A **72**, 023406 (2005).
[20] M. F. Andersen, A. Kaplan, and N. Davidson, Phys. Rev. Lett. **90**, 023001 (2003).
[21] A. Derevianko, Phys. Rev. Lett. **105**, 033002 (2010).
[22] R. Chicireanu et al., Phys. Rev. Lett. **106**, 063002 (2011).
[23] A. Kaplan, M. F. Andersen, and N. Davidson, Phys. Rev. A **66**, 045401 (2002).
[24] P. Wolf et al., Phys. Rev. A **75**, 063608 (2007).
[25] N. Poli et al., Phys. Rev. Lett. **106**, 038501 (2011).
[26] A. Peters et al., Metrologia **38**, 25 (2001).
[27] M. Karski et al., New J. Phys. **12**, 065027 (2010).
[28] L. Yi et al., Phys. Rev. Lett. **106**, 073005 (2011).